INTERNATIONAL JOURNAL FOR NUMERICAL METHODS IN FLUIDS
Int. J. Numer. Meth. Fluids 2008; **58**:1287–1298
Published online 14 April 2008 in Wiley InterScience (www.interscience.wiley.com). DOI: 10.1002/fld.1814

High accuracy time and space transform method for advection–diffusion equation in an unbounded domain

Suqin Chen*, †, Xionghua Wu, Yingwei Wang and Weibin Kong

Department of Mathematics, Tongji University, Siping Road No. 1239, Shanghai 200092, People's Republic of China

SUMMARY

A new numerical method called high accuracy time and space transform method (TSTM) is introduced to solve the advection–diffusion equation in an unbounded domain. By a spatial transform, the advection–diffusion equation in the unbounded domain R^n is converted to one on the bounded domain $[-1, 1]^n$, and the Laplace transform is applied to eliminate time dependency. The consequent boundary value problem is solved by collocation on Chebyshev points. To face the well-known computational challenge represented by the numerical inversion of the Laplace transform, Talbot's method is applied, consisting of numerically integrating the Bromwich integral on a special contour by means of trapezoidal or midpoint rules. Numerical experiments illustrate that TSTM has exponential rate in time and space. Copyright © 2008 John Wiley & Sons, Ltd.

Received 19 July 2007; Revised 27 February 2008; Accepted 28 February 2008

KEY WORDS: advection–diffusion equation; unbounded domain; rational collocation method; the Laplace transform; Talbot's method and numerical inversion

1. INTRODUCTION

Numerically solving the advection–diffusion equation in an unbounded domain is of crucial interest in such different areas as fluid dynamics, geophysics, and plasma physics.

When computing the solution of an advection–diffusion equation in the unbounded domain, one usually introduces artificial boundaries. In order to limit the computational cost, these boundaries must be chosen not too far from the domain of interest. Therefore, the boundary conditions must be

*Correspondence to: Suqin Chen, Department of Mathematics, Tongji University, Siping Road No. 1239, Shanghai 200092, People's Republic of China.
†E-mail: tjchensuqin@mail.tongji.edu.cn

Contract/grant sponsor: National Nature Science Foundation of China; contract/grant numbers: 10671146, 50678122

good approximations to the so-called 'transparent' boundary condition (i.e. such that the solution of the problem in the bounded domain is equal to the solution in the original domain). When artificial boundary conditions are introduced, one must take into consideration two problems: first, do they lead to a well-posed boundary value problem (BVP)? Second, is the error between the solutions to the original problem and the resulting BVP as small as possible in the computational domain? Some papers [1, 2] deal with these problems.

For the advection–diffusion equation in a bounded domain, the finite volume method (FVM) [3, 4], combined finite element–finite volume method [5, 6], and discontinuous Galerkin method [7, 8] are widely used. However, for some problems, (e.g. diffusion of a Gaussian hill in uniformly rotating flow field), a large number of meshes that cover the large computational domain lead to huge central processing unit (CPU) time, and computational precision is not high [6].

For the time-dependent linear PDE, Runge–Kutta and linear multistep formulas are usually to be chosen as a time-marching method. The drawback of these methods is error cumulation. The Laplace transform is a technique proposed early, which removes the time dependency and converts the problem into a BVP. However, this approach never really became popular in computational work. The main reason may be that the Laplace transform, particularly its numerical inversion, has a reputation for being a computational challenge for the fact that the numerical inversion of the Laplace transform is an ill-posed problem when the transform is known only as a real-valued function. Recently, Talbot's method [9] has become a very popular technique for numerical inversion of the Laplace transform. The technique combines the trapezoid rule or the midpoint rule with contour integration by using complex arithmetic. The convergence rates for these optimized quadrature formulas are very fast: roughly $O(3^{-M})$ [10], where M is the number of sample points. Additionally, unlike the traditional time-marching method, an interesting advantage of using the Laplace transform is that it is easily parallelizable.

Collocation methods based on rational interpolation have been developed by Berrut and his collaborators [11–13]. The method is based on rational interpolation in barycentric form with prescribed barycentric weights and transformed Chebyshev points. Berrut and Mittelmann [14] applied the rational interpolation with tan transform for approximation of functions with a large gradient in the center of the interval. Their methods required that the underlying problem be transformed to new coordinates. Tee and Trefethen [15] developed a new rational collocation method based on a sinh function, which does not require that the underlying problem be transformed into new coordinates and need not take into consideration singularities of the underlying solution. They applied the method to the blow-up and moving front problems and achieved high accuracy results.

It can be seen that in the traditional numerical method to solve an advection–diffusion equation in the unbounded domain, there exist two difficult points: space discretizion in the unbounded domain and error cumulation in a time-marching method such as Runge–Kutta and linear multistep methods.

In this paper, a new numerical method called high accuracy time and space transform method (TSTM) is introduced to deal with the two difficult points mentioned above. We first introduce a transform to convert the infinite domain R^n to $[-1, 1]^n$, avoiding the artificial boundary conditions problem. For the transformed equation on $[-1, 1]^n$, the rational interpolation in barycentric form with prescribed barycentric weights and Chebyshev points is applied. For time-dependent linear PDE, the Laplace transform is used, avoiding error cumulation in the traditional time-marching method. Numerical experiments show that TSTM has two advantages: the first advantage has exponential convergence rate in time and space; the second advantage is that a transform to be

DOI: 10.1002/fld

introduced for the advection–diffusion equation in infinite domain avoids the artificial boundary problems.

The paper is constructed as follows: in Section 2, a transform is used to convert a class of PDE in infinite domain R^n to PDE in $[-1,1]^n$. In Section 3, we use the Laplace transform to convert a class of time-dependent linear PDEs to BVPs. In Section 4, we give a short review of the rational collocation method based on barycentric formula. In Section 5, we employ Talbot's method for the numerical inversion of the Laplace transform. In Section 6, we test one example involving diffusion of a Gaussian hill. Section 7 gives a brief conclusion.

2. A SPACE TRANSFORM FOR PDE IN THE INFINITE DOMAIN

In this paper, we focus on the two-dimensional time-dependent linear PDE of the form

$$\begin{gathered}\frac{\partial u}{\partial t}=a(x,y)\frac{\partial^2 u}{\partial x^2}+b(x,y)\frac{\partial^2 u}{\partial x\partial y}+c(x,y)\frac{\partial^2 u}{\partial y^2}+d(x,y)\frac{\partial u}{\partial x}+e(x,y)\frac{\partial u}{\partial y}+h(x,y)u\\ u(x,y,0)=u_0(x,y)\\ \lim_{r\to\infty}u(x,y,t)=0,\quad r=\sqrt{x^2+y^2},\quad (x,y)\in R^2,\ \ t\in(0,+\infty)\end{gathered}\tag{1}$$

where $a(x,y), b(x,y), c(x,y), d(x,y), e(x,y), h(x,y), u_0(x,y)$ are continuous in R^2.

For (1), we introduce the following transform:

$$\begin{aligned}\xi&=\frac{e^{x/l_x}-1}{e^{x/l_x}+1}\\ \eta&=\frac{e^{y/l_y}-1}{e^{y/l_y}+1}\end{aligned}\tag{2}$$

where l_x and l_y are parameters determined by the underlying problem. Equation (1) can be converted to the following equation:

$$\frac{\partial u}{\partial t}=\widetilde{a(\xi,\eta)}\frac{\partial^2 u}{\partial \xi^2}+\widetilde{b(\xi,\eta)}\frac{\partial^2 u}{\partial \xi\partial\eta}+\widetilde{c(\xi,\eta)}\frac{\partial^2 u}{\partial \eta^2}+\widetilde{d(\xi,\eta)}\frac{\partial u}{\partial \xi}+\widetilde{e(\xi,\eta)}\frac{\partial u}{\partial \eta}+\widetilde{h(\xi,\eta)}u$$

$$u(\xi,\eta,0)=u_0(\xi,\eta)\tag{3}$$

$$u|_\Gamma=0,\quad \Gamma=\partial\Omega,\quad \Omega=[-1,1]\times[-1,1]\tag{4}$$

$$(\xi,\eta)\in[-1,1]\times[-1,1]$$

After numerically solving (3)–(4) in the bounded domain, the inversion of the transform

$$\begin{aligned}x&=l_x\log\left(\frac{1+\xi}{1-\xi}\right)\\ y&=l_y\log\left(\frac{1+\eta}{1-\eta}\right)\end{aligned}\tag{5}$$

is used to convert the solution of (3)–(4) to the solution in the original domain.

DOI: 10.1002/fld

A similar transform can be presented in 1D and 3D problems; without loss of generality, we take into consideration the above 2D problem.

3. THE LAPLACE TRANSFORM FOR TIME-DEPENDENT LINEAR PDE

Let $u(t)$ be a piece-wise continuous function of exponential growth on $[0,\infty)$. The Laplace transform $\widehat{u}$ of u is defined by

$$\widehat{u}(s)=\int_0^\infty \mathrm{e}^{-st}u(t)\,\mathrm{d}t$$

To solve the IBVP (3)–(4), we take the Laplace transform of u giving $\widehat{u}$ as the solution to

$$s\widehat{u}-u_0(\xi,\eta)=\widetilde{a(\xi,\eta)}\frac{\partial^2\widehat{u}}{\partial\xi^2}+\widetilde{b(\xi,\eta)}\frac{\partial^2\widehat{u}}{\partial\xi\partial\eta}+\widetilde{c(\xi,\eta)}\frac{\partial^2\widehat{u}}{\partial\eta^2}+\widetilde{d(\xi,\eta)}\frac{\partial\widehat{u}}{\partial\xi}+\widetilde{e(\xi,\eta)}\frac{\partial\widehat{u}}{\partial\eta}+\widetilde{h(\xi,\eta)}\widehat{u}$$

Defining $\widetilde{f(\xi,\eta,s)}=\widetilde{h(\xi,\eta)}-s$, $\widetilde{g(\xi,\eta)}=-u_0(\xi,\eta)$, $\widehat{u}$ satisfies

$$\widetilde{a(\xi,\eta)}\frac{\partial^2\widehat{u}}{\partial\xi^2}+\widetilde{b(\xi,\eta)}\frac{\partial^2\widehat{u}}{\partial\xi\partial\eta}+\widetilde{c(\xi,\eta)}\frac{\partial^2\widehat{u}}{\partial\eta^2}+\widetilde{d(\xi,\eta)}\frac{\partial\widehat{u}}{\partial\xi}+\widetilde{e(\xi,\eta)}\frac{\partial\widehat{u}}{\partial\eta}+\widetilde{f(\xi,\eta,s)}\widehat{u}=\widetilde{g(\xi,\eta)} \tag{6}$$

Similarly, taking the Laplace transform of the boundary conditions gives

$$\widehat{u}|_\Gamma=0,\quad \Gamma=\partial\Omega,\quad \Omega=[-1,1]\times[-1,1] \tag{7}$$

For numerical purposes, (6)–(7) are solved for a sequence of value of $\{s_n\}$, and then a numerical inversion Laplace transform to $\{\widehat{u}(\xi,\eta,s_n)\}$ is applied.

4. THE RATIONAL COLLOCATION METHOD BASED ON BARYCENTRIC FORM FOR BVP (6)–(7)

We now introduce the rational collocation method based on barycentric interpolation [11]. The barycentric form of a rational function $p_N(x)$ that interpolates data $u_0,u_1,\ldots,u_N$ at points $x_0,x_1,\ldots,x_N$ is

$$p_N(x)=\frac{\sum_{k=0}^N \dfrac{\omega_k}{x-x_k}u_k}{\sum_{k=0}^N \dfrac{\omega_k}{x-x_k}} \tag{8}$$

where ω_k, $k=0,\ldots,N$, are called barycentric weights. An advantage of representing a rational interpolant in barycentric form is the simplicity of its derivatives formulae at x_j. The nth derivative of $p_N(x)$ at x_j can be expressed as $p_N^{(n)}(x_j)=\sum_{k=0}^N D_{jk}^{(n)}u_k$. The elements of $D^{(1)}$ and $D^{(2)}$, that

DOI: 10.1002/fld

is, first- and second-order differential matrices, are given by

$$D_{jk}^{(1)}=\begin{cases}\dfrac{\omega_k}{\omega_j(x_j-x_k)} & \text{if } j\neq k\\ -\displaystyle\sum_{i\neq j} D_{ji}^{(1)} & \text{if } j=k\end{cases} \tag{9}$$

$$D_{jk}^{(2)}=\begin{cases}2D_{jk}^{(1)}\left(D_{jj}^{(1)}-\dfrac{1}{x_j-x_k}\right) & \text{if } j\neq k\\ -\displaystyle\sum_{i\neq j} D_{ji}^{(2)} & \text{if } j=k\end{cases} \tag{10}$$

When $x_k=\cos(k\pi/N)$ are Chebyshev points of the second kind, $\omega_0=\frac{1}{2}, \omega_k=(-1)^k, k=1,\ldots,N-1, \omega_N=(-1)^N/2$, the above formulae are the differential matrices in the Chebyshev collocation method [16].

The Lagrange polynomial interpolations can be represented in barycentric form [12], which are stable and have a special, beautiful symmetry. A rational interpolation can be made from polynomial interpolation in barycentric form by modifying its points and leaving its barycentric weights unchanged.

The rational interpolation based on barycentric form with the transformed Chebyshev points has the following convergence analysis.

Theorem 4.1 (*Berrut et al.* [*11*])
Let D_1 and D_2 be domains in $\mathbb{C}$ containing $J=[-1,1]$ and a real interval I, respectively. Let $g: D_1\to D_2$ be a conformal map such that $g(J)=I$. If $u: D_2\to\mathbb{C}$ is a function such that the composition $u\circ g: D_1\to\mathbb{C}$ is analytic inside and on an ellipse $E_\rho, \rho>1$, with foci at ±1 and the sum of its semi-major and semi-minor axes is equal to ρ. Let $P_N(x)$ be the rational function (8) interpolating u between the transformed Chebyshev points $x_k=g(\cos(k\pi/N))$ with barycentric weights $\omega_0=1/2, \omega_k=(-1)^k, k=1,\ldots,N-1, \omega_N=(-1)^N/2$. Then, for every $x\in[-1,1]$,

$$|p_N(x)-u(x)|=O(\rho^{-N}) \tag{11}$$

It can be seen from Theorem 4.1 that rational interpolation preserves exponential convergence when interpolated at transformed Chebyshev points.

For BVP (6)–(7), let the collocation points be

$$X=\{(\xi_k,\eta_l)|k=0,\ldots,N, l=0,\ldots,N\}$$

Define

$$\widetilde{A}=\{\widetilde{a(\xi_k,\eta_l)}\}_{k=0,\ldots,N;l=0,\ldots,N},\quad \widetilde{B}=\{\widetilde{b(\xi_k,\eta_l)}\}_{k=0,\ldots,N;l=0,\ldots,N}$$

$$\widetilde{C}=\{\widetilde{c(\xi_k,\eta_l)}\}_{k=0,\ldots,N;l=0,\ldots,N},\quad \widetilde{D}=\{\widetilde{d(\xi_k,\eta_l)}\}_{k=0,\ldots,N;l=0,\ldots,N}$$

$$\widetilde{E}=\{\widetilde{e(\xi_k,\eta_l)}\}_{k=0,\ldots,N;l=0,\ldots,N},\quad \widetilde{F}=\{\widetilde{f(\xi_k,\eta_l,s)}\}_{k=0,\ldots,N;l=0,\ldots,N}$$

$$\widetilde{G}=\{\widetilde{g(\xi_k,\eta_l)}\}_{k=0,\ldots,N;l=0,\ldots,N}$$

DOI: 10.1002/fld

By stripping the first-order differential matrix $D^{(1)}$, second-order differential matrix $D^{(2)}$, and the identity matrices, $\widetilde{A}, \widetilde{B}, \widetilde{C}, \widetilde{D}, \widetilde{E}, \widetilde{F}, \widetilde{G}$ of their first and last rows, respectively, we obtain $(N-1)\times(N-1)$ matrices $D_1, D_2, I, A, B, C, D, E, F, G$. Discretizing the BVP at points (ξ_k, η_l) for $k=1,\ldots,N-1, l=1,\ldots,N-1$, yields

$$A\circ(D_2\widehat{U}(s_n))+B\circ(D_1\widehat{U}(s_n)D_1^{\mathrm{T}})+C\circ(\widehat{U}(s_n)D_2^{\mathrm{T}})+D\circ(D_1\widehat{U}(s_n))$$
$$+E\circ(\widehat{U}(s_n)D_1^{\mathrm{T}})+F\circ\widehat{U}(s_n)=G \tag{12}$$

where the unknown $\widehat{U}(s_n)$ is a matrix of size $(N-1)\times(N-1)$ with $\widehat{u}_{k,l}(s_n)$ evaluating $\widehat{u}(\xi_k,\eta_l,s_n), k=1,\ldots,N-1, l=1,\ldots,N-1$; $\circ$ denotes the Hadamard product of matrices. Combining the boundary conditions and solving Equation (12), one can obtain the numerical solution $\widehat{U}(s_n)$.

5. NUMERICAL INVERSION OF THE LAPLACE TRANSFORM

The Laplace transform represents a very effective tool for solving several problems in the fields of science and engineering; however, the numerical inversion of the Laplace transform still remains a difficult problem. In recent years, many results have been obtained in the field of numerical inversion. Among them, a very accurate and general method is given by Talbot [9]. Talbot's method has proved to be applicable both to a wide range of Laplace transform functions and to a wide range of values of t where we need to compute $f(t)$. In addition, the method has exponential convergence rate under certain circumstances [10]. In this section, we will apply Talbot's method to obtain the approximation of $u(\xi,\eta,t)$ based on the sequence $\{\widehat{u}(\xi,\eta,s_n)\}$.

The inversion Laplace transform of $\widehat{u}$ is defined by

$$u(\xi,\eta,t)=\frac{1}{2\pi\mathrm{i}}\int_B \mathrm{e}^{st}\widehat{u}(\xi,\eta,s)\,\mathrm{d}s \tag{13}$$

which is called the Bromwich integral, with B being the Bromwich line $\mathrm{Re}(s)=\sigma>\sigma_0$. σ_0 is the maximum value of the real part of all singularities of $\widehat{u}$.

In Talbot's method, the Bromwich line is deformed into a curve Γ that begins and ends in the left half-plane, such that $\mathrm{Re}(s)\to-\infty$ on the contour. Owing to the exponential factor e^{st}, the integrand decays rapidly on such a contour. Talbot's contour is parameterized by

$$\Gamma: s(\theta)=\sigma+\mu(\theta\cot\theta+\nu\mathrm{i}\theta),\quad -\pi\leqslant\theta\leqslant\pi \tag{14}$$

where σ, μ, and ν are real parameters that determine the geometry of the curve. Both μ and ν are positive. We assume that Γ lies in the region of analyticity of $\widehat{u}$. Using the Cauchy Integral Theorem and (14), the Bromwich integral (13) can be expressed as

$$u(\xi,\eta,t)=\frac{1}{2\pi\mathrm{i}}\int_B \mathrm{e}^{st}\widehat{u}(\xi,\eta,s)\,\mathrm{d}s=\frac{1}{2\pi\mathrm{i}}\int_{-\pi}^{\pi}\mathrm{e}^{s(\theta)t}\widehat{u}(\xi,\eta,s(\theta))s'(\theta)\,\mathrm{d}\theta \tag{15}$$

where $s'(\theta)=\mu(\cot\theta-\theta\csc^2\theta+\nu\mathrm{i})$. The above integral can be approximated by the trapezoidal rule or the midpoint rule. Here, we use the midpoint rule with an even number of intervals, say $2M$, as used in [9].

DOI: 10.1002/fld

The grid is defined as

$$\theta_n = (2n+1)\frac{\pi}{2M}, \quad n = -M, \ldots, M-1 \tag{16}$$

Denote the approximation to (15) by

$$u_M(\xi, \eta, t) = \frac{1}{2Mi} \sum_{n=-M}^{M-1} \mathrm{e}^{s(\theta_n)t} s'(\theta_n) \widehat{u}(\xi, \eta, s(\theta_n)) \tag{17}$$

or

$$u_M(\xi, \eta, t) = \mathrm{Im}\left(\frac{1}{2M} \sum_{n=-M}^{M-1} \mathrm{e}^{s(\theta_n)t} s'(\theta_n) \widehat{u}(\xi, \eta, s(\theta_n)) \right) \tag{18}$$

If symmetry is used, let $s_n = s(\theta_n), s'_n = s'(\theta_n)$; we can obtain the approximation to $u(\xi, \eta, t)$, i.e.

$$u_M(\xi, \eta, t) = \mathrm{Im}\left(\frac{1}{M} \sum_{n=0}^{M-1} \mathrm{e}^{s_n t} s'_n \widehat{u}(\xi, \eta, s_n) \right) \tag{19}$$

Here, $\widehat{u}(\xi, \eta, s_n)$ are solved from (12).

It is well known that Talbot's method (14) with fixed parameters converges at a subgeometric rate of $O(\mathrm{e}^{-c\sqrt{M}})$; see [9]. Weideman [10] let both σ and μ be proportional to the ratio M/t; a geometric rate $O(\mathrm{e}^{-cM})$ as $M \to \infty$ can be obtained. Moreover, Weideman finds optimal parameters for Talbot's method for some problems: when the following Talbot's contour

$$\Gamma : s(\theta) = \frac{M}{t}(-0.2407 + 0.2378\theta \cot(0.7409\theta) + 0.1349\mathrm{i}\theta) \tag{20}$$

is used as the Bromwich line, the convergence rate is given by $O(\mathrm{e}^{-2.56M})$.

6. NUMERICAL EXAMPLE

In this section, we present one example involving diffusion of a Gaussian hill, as studied by Wang and Liu [6] and Pudykiewicz and Staniforth [17], illustrating our methodology.

The diffusion of a Gaussian hill in a uniformly rotating flow field is controlled by the following equation:

$$u_t + (-\Omega y)u_x + (\Omega x)u_y = K(u_{xx} + u_{yy})$$

$$u(x, y, 0) = A_0 \exp\left\{ -\left[\frac{(x-x_0)^2 + (y-y_0)^2}{2\sigma^2} \right] \right\} \tag{21}$$

where K and σ are constants, $-\Omega y$ and Ωx are the components of the velocity field that has a constant positive angular velocity of $\Omega = 10^{-5}\,\mathrm{s}^{-1}$ about the central point of the plane. For

DOI: 10.1002/fld

the parameters of the experiments, we choose $A_0=100$ units, $\sigma^2=2\times10^{10}$, $(x_0, y_0)=(8\times10^5, 16\times10^5)$, and four different representative values for K, namely,

(i) $K=10^2\,\mathrm{m^2\,s^{-1}}$ (an advection-dominant problem),
(ii) $K=10^4\,\mathrm{m^2\,s^{-1}}$ (as a very stable situation and typical of high-pressure systems),
(iii) $K=5\times10^4\,\mathrm{m^2\,s^{-1}}$ (a moderately unstable situation),
(iv) $K=7\times10^4\,\mathrm{m^2\,s^{-1}}$ (intensive subgrid-scale mixing).

In an infinite plane, the analytic solution of (21) is given by

$$u(x,y,t)=\frac{A_0}{1+2Kt/\sigma^2}\exp\left\{-\left[\frac{\widetilde{x}^2+\widetilde{y}^2}{2(\sigma^2+2Kt)}\right]\right\} \tag{22}$$

where $\widetilde{x}=x-x_0\cos\Omega t+y_0\sin\Omega t$ and $\widetilde{y}=y-x_0\sin\Omega t-y_0\cos\Omega t$.

For this problem, parameters l_x and l_y in transform (2) are set as follows: $l_x=l_y=8\times10^5$. Using transform (2), (21) in infinite plane is converted to a PDE in $[-1,1]\times[-1,1]$. The number of Chebyshev points is set as $N=48$ in Section 4. We take $M=16$ in (19). s_n is taken as discussed in the last section. For each s_n, $\widehat{u}(\xi,\eta,s_n)$ can be obtained as discussed in Section 3; then applying Talbot's method, we can obtain the evaluation $u(\xi,\eta,t)$, and then using the inversion of the transform in Section 2, we can obtain the evaluation $u(x,y,t)$.

When assessing the performance of a method, two important criteria are the accuracy and efficiency. For the numerical experiments, the following terms are used to compare the performance of the scheme's accuracy: the error of central value

$$\mathrm{abs}(u_{\mathrm{e\ central}}-u_{\mathrm{n\ central}}) \tag{23}$$

The L_2 error norm

$$\frac{\|u_{\mathrm{e}}(X)-u_{\mathrm{n}}(X)\|_2}{\|u_{\mathrm{e}}(X)\|_2} \tag{24}$$

where $u_{\mathrm{e}}(X)$ and $u_{\mathrm{n}}(X)$ are the exact solution and the numerical solution on collocation points, respectively. The ratios of CPU times of different numerical methods are used to evaluate the efficiency of the TSTM scheme.

The error of central value compares the error of the numerical and exact solutions at the maximum value point of the solution; the L_2 error norm gives the root-mean-square percent error of the numerical and exact solutions. The ideal scheme should yield error of central value and L_2 error of zero.

Similar to [6, 17], the simulation results after one rotation with $K=10^4$, 5×10^4, and 7×10^4 are investigated and compared. In addition, the simulation result with $K=10^2$ is also given.

The results after one rotation are shown in Table I and in Figures 1–4.

It is necessary to point out that in Table I, the computations using the full FVM and the discontinuous Galerkin method (DGM) are carried out on a mesh with 9494 triangular cells and 4876 nodes, computations using the combined finite volume–finite element (FV–FE) method are carried out on a mesh with 14 838 triangular cells and 7580 nodes, whereas computations using TSTM proposed by this paper are carried out on collocation points $N\times N$ $(N=48)$.

It can be seen that from Table I, the accuracy of the method proposed by this paper is superior to that of the other three schemes. Isolines of the error field (exact solution minus numerical solution) are symmetric about the central value point, which differs from the FV–FE method, full

DOI: 10.1002/fld

Table I. Central values and errors of the Gaussian hill after one rotation.

K (m^2s^{-1})	Exact result (central value)	Scheme	Cells	Numerical result (central value)	The error of central value	L_2 error norm	Ratio of CPU time
1×10^4	61.414	FV–FE [6]	14 838	63.9	2.5	5.098e−01	0.5510
		FVM [6]	9494	55.7	5.7	5.099e−01	0.7494
		DG [6]	9494	64.6	3.2		4.1711
		TSTM	48×48	61.414	5.781e−06	3.633e−06	1.0
5×10^4	24.145	FV–FE [6]	14 838	43.6	9.5	7.791e−02	0.2641
		FVM [6]	9494	23.7	0.4	7.723e−02	0.6971
		DG [6]	9494	42.9	8.8		5.2893
		TSTM	48×48	24.145	7.072e−09	8.648e−06	1.0
7×10^4	18.525	FV–FE [6]	14 838	37.4	8.9	7.303e−02	0.2384
		FVM [6]	9494	18.3	0.2	6.372e−02	0.8656
		DG [6]	9494	37.1	8.6		4.7608
		TSTM	48×48	18.525	2.793e−09	1.496e−05	1.0

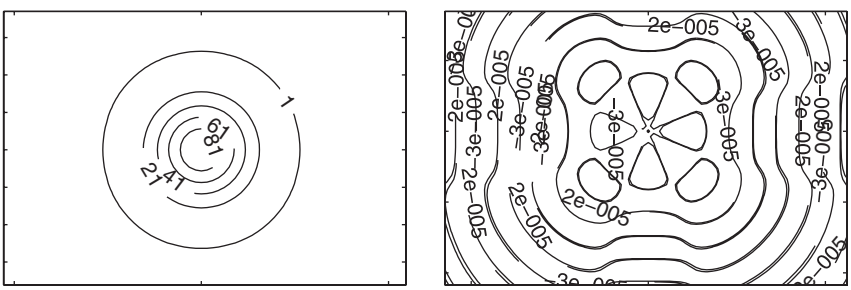

Figure 1. With diffusion coefficient $K=100$. Left part: isolines of the Gaussian hill after one rotation. Right part: isolines of the error field (exact solution minus numerical solution).

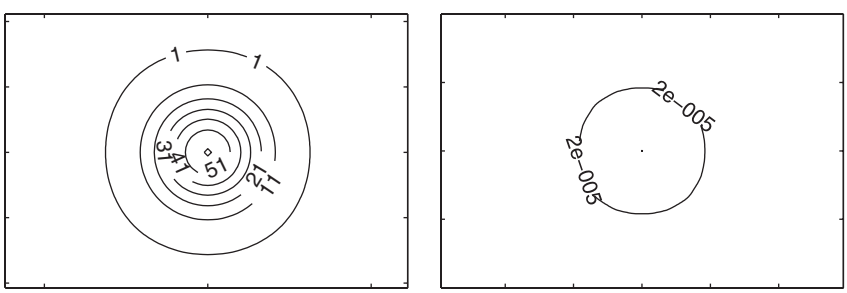

Figure 2. With diffusion coefficient $K=10^4$. Left part: isolines of the Gaussian hill after one rotation. Right part: isolines of the error field (exact solution minus numerical solution).

DOI: 10.1002/fld

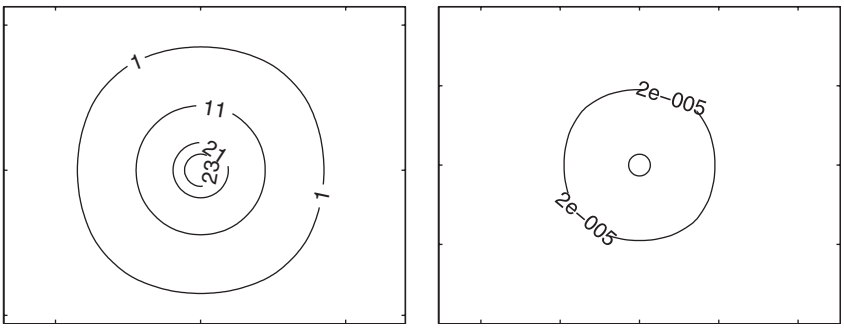

Figure 3. With diffusion coefficient $K = 5 \times 10^4$. Left part: isolines of the Gaussian hill after one rotation. Right part: isolines of the error field (exact solution minus numerical solution).

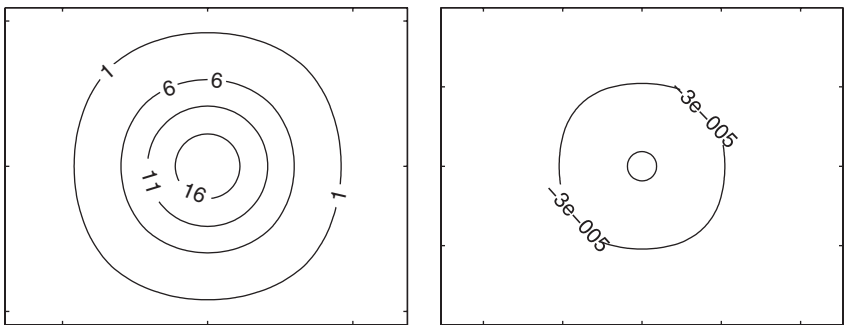

Figure 4. With diffusion coefficient $K = 7 \times 10^4$. Left part: isolines of the Gaussian hill after one rotation. Right part: isolines of the error field (exact solution minus numerical solution).

FVM, and DGM [6]. In addition, ratios of CPU times of different numerical methods show that the computational cost of TSTM is higher than that of the FV–FE method, full FVM, and lower than that of DGM. In particular, for larger diffusion coefficients, the computational cost of TSTM is a little higher than that of the FV–FE method, but there is a larger advantage in accuracy for TSTM.

The diffusion of a Gaussian hill with diffusion coefficient $K = 10^2$ is an advection-dominant problem with a central value = 99.376. Numerically solving the case is a more challenging topic; Wang and Liu [6] and Pudykiewicz and Staniforth [17] did not deal with the case. We apply TSTM to the case in which the collocation points are also 48×48, the error of central value is 2.639e − 05, and the L_2 error norm is 2.357e − 05. High precision for the advection-dominant problem is again gained.

Moreover, simulation results after one rotation with $K = 10^2$, 10^4, 5×10^4, and 7×10^4 carried out on collocation points having different point numbers $N = 20, 25, 30, 35, 40, 44, 48$ are shown in Figure 5, where N are collocation point numbers. In addition, we can see that the method can achieve exponential convergence rates.

DOI: 10.1002/fld

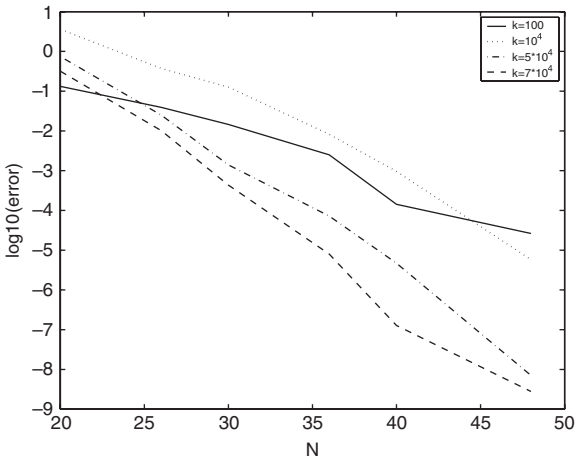

Figure 5. log 10(error) at after 1 rotation for N increase.

7. CONCLUSION

We have presented a very accurate method TSTM that far outperforms the FV–FE method, full FVM, and DGM for advection–diffusion equation in the infinite domain. It combines ideas from the existing rational spectral collocation method with the numerical inversion technique of the Laplace transform using Talbot's method. We are in the process of investigating further improvements of this method as well as its application to some advection–diffusion problems with time-dependent coefficients in the unbounded domain.

ACKNOWLEDGEMENTS

The support from the National Nature Science Foundation of China (No. 10671146, 50678122) is fully acknowledged. The authors thank the referees for their useful comments and suggestions.

REFERENCES

1. Filatov DM. Splitting as an approach to constructing local exact artificial boundary conditions. *Applied Mathematics and Computation* 2005; **170**:1209–1242.
2. Halpern L. Artificial boundary conditions for the linear advection diffusion equation. *Mathematics of Computation* 1986; **46**(174):425–438.
3. Barth TJ, Jespersen DC. The design and application of upwind schemes on unstructured meshes. *AIAA Paper 89-0366*, 1989.
4. Anastasiou K, Chan CT. Solution of the 2D shallow water equations using the finite volume method on unstructured triangular meshes. *International Journal for Numerical Methods in Fluids* 1997; **24**:1225–1245.
5. Feistauer M, Felcman J, Lukacova-Medvidova M. Combined finite element–finite volume solution of compressible flow. *Journal of Computational and Applied Mathematics* 1995; **63**:179–199.
6. Wang JW, Liu RX. Combined finite volume–finite element method for shallow water equations. *Computers and Fluids* 2005; **34**:1199–1222.
7. Cockburn B, Shu CW. The local discontinuous Galerkin method for time-dependent convection–diffusion systems. *SIAM Journal on Numerical Analysis* 1998; **35**(6):2440–2463.

DOI: 10.1002/fld

8. Aizinge V, Dawson C. A discontinuous Galerkin method for two-dimensional flow and transport in shallow water. *Advances in Water Resources* 2002; **25**:67–84.
9. Talbot A. The accurate numerical inversion of Laplace transforms. *Journal of the Institute of Mathematics and its Applications* 1979; **23**:97–120.
10. Weideman JAC. Optimizing Talbot's contours for the inversion of the Laplace Transform. *SIAM Journal on Numerical Analysis* 2006; **44**:2342–2362.
11. Berrut JP, Baltensperger R, Mittelmann HD. Recent developments in barycentric rational interpolation. *International Series of Numerical Mathematics* 2005; **15**:27–51.
12. Berrut JP, Trefethen LN. Barycentric Lagrange interpolation. *SIAM Review* 2004; **46**:501–517.
13. Baltensperger R, Berrut JP, Noel B. Exponential convergence of a linear rational interpolant between transformed Chebychev points. *Mathematics of Computation* 1999; **68**:1109–1120.
14. Berrut JP, Mittelmann HD. Adaptive point shifts in rational approximation with optimized denominator. *Journal of Computational and Applied Mathematics* 2004; **81–92**:164–165.
15. Tee TW, Trefethen LN. A rational spectral collocation method with adaptively transformed Chebyshev grid points. *SIAM Journal on Scientific Computation* 2006; **28**:1798–1811.
16. Trefethen LN. *Spectral Methods in Matlab*. SIAM: Philadelphia, PA, 2000.
17. Pudykiewicz J, Staniforth A. Some properties and comparative performance of the semi-Lagrangian method of Robert in the solution of the advection–diffusion equation. *Atmosphere Ocean* 1984; **22**:283–308.

DOI: 10.1002/fld